PHYSICAL REVIEW C VOLUME 8, NUMBER 2 AUGUST 1973

$^4He(\gamma, p)t$ Reaction for Photon Energies Between 180 and 320 MeV*

S. E. Kiergan,† A. O. Hanson, and L. J. Koester, Jr.
Physics Department, University of Illinois, Urbana, Illinois 61801
(Received 3 April 1972; revised manuscript received 1 May 1973)

The differential cross section for the reaction $^4He(\gamma, p)t$ was measured in a spark chamber experiment for photon energies between 180 and 320 MeV and proton c.m. angles between 60 and 120°. The results show that the cross section continues to decline with increasing energy. No evidence of a peak was found in the region of the first pion-nucleon resonance. An empirical function, involving the nucleon momentum distribution in the nucleus, was derived from a simple model of the photodisintegration process, and was used to correlate the observed differential cross sections over a large range of energy and angle.

INTRODUCTION

The reaction $^4He(\gamma,p)t$ has been studied by a number of authors, with most of the theoretical and experimental work concentrating on the energy region of the dipole resonance. A review of work on this reaction and its inverse, in this energy range, has been presented by Meyerhof and Fiarman.[1] A study of the inverse reaction at an energy equivalent to 137-MeV photons has been made by Didelez *et al.*[2] using 156-MeV protons on a tritium target. Gorbunov[3] and Stenberg[4] have studied the photoproton process to energies slightly above pion threshold. At higher energies, there has been little information available on this cross section, although a number of experiments have measured the photoproton production from the main photodisintegration cross section in this energy region, the so-called quasideuteron effect. Recently, Picozza *et al.*[5] have reported measurements of the 90° cross section for the energy range between 200 and 450 MeV.

The energy region between pion threshold and the first pion-nucleon resonance is of interest in this reaction because it is here that one would expect to find evidence of mesonic effects on the cross section if they play a major role in the two body photodisintegration of ^4He. In this energy region the deuteron photodisintegration cross section displays a broad maximum ascribed to production and reabsorption of pions in the deuteron.

In this paper we will present the results of a measurement of the $^4He(\gamma,p)t$ cross section for photon energies between 180 and 320 MeV at angles between 60 and 120° in the c.m. system. In addition we will calculate the angular distribution of the emitted protons on the basis of a semiempirical determination of a function of the momentum distribution of the nucleons in the ^4He nucleus and compare this with the observed angular distribution.

EXPERIMENTAL ARRANGEMENT

The experimental layout is shown in Fig. 1. A 320-MeV bremsstrahlung beam from the University of Illinois 340-MeV betatron was used to irradiate a target cell filled with liquid ^4He. Downstream from the target, the beam energy was measured by a Wilson quantameter. The target cell was a cylinder 3.18 cm in diameter constructed of 0.038-mm Mylar film.

Particles emerging from the target entered an array of scintillation counters and optical spark chambers designed to measure the range and angle of the protons and the angle of the tritons produced from $^4He(\gamma,p)t$ reactions in the target cell. A proton exiting from the target passed through a pair of thin-foil spark chambers, a layer of brass absorber, and a pair of scintillation counters, and was stopped in a large spark chamber which had 21 aluminum plates 3.2 mm thick. The triton associated with the proton passed through two thin-foil spark chambers and was stopped in a scintillation counter.

The apparatus accepted protons with laboratory angles between 50 and 120° and tritons whose laboratory angle was between 40 and 110°. The acceptance limit on azimuthal angle for both tritons and protons was ±25° from the horizontal plane. Allowing necessary margins for finite target size and scattering, the apparatus could accept all $^4He(\gamma,p)t$ events with c.m. angle between 60 and 120° and azimuthal angle within 20° of the horizontal for proton energies between 180 and 320 MeV.

The presence of a possible $^4He(\gamma,p)t$ event was signaled by coincident pulses from two of the proton scintillation counters and one of the triton counters. Such coincident pulses were sensed by the University of Illinois fast electronic logic circuitry which fired the spark chambers. An overhead camera photographed the spark chamber tracks both directly and through mirrors located at the downstream end of the chambers.

The division between the triton counters at 60° and the division between the second row of proton counters at 82° was made in order to prevent the triggering of the apparatus by the quasifree production of negative pions from neutrons in the ^{4}He. The kinematics of the $^4\mathrm{He}(\gamma, p)t$ reaction require that the angle of the proton be greater than 82° when the triton angle is less than 60°, while the kinematics of the $n(\gamma, \pi^-)p$ reaction restricted such events to the downstream proton and triton counters. Consequently, the electronic logic was arranged so as not to respond to coincidences involving the downstream triton counter and the downstream proton counter.

The range of the protons was such that the highest-energy protons could not be stopped if the absorber in front of the thick-plate chamber was thin enough to allow the protons from 180-MeV-proton-energy $^4\mathrm{He}(\gamma, p)t$ events to enter the chamber. Therefore, the appratus was run in two configurations. In the first configuration the absorber was thin enough to allow the protons from the lowest-photon-energy events to enter the thick-plate chamber, and the last gap of the chamber was used as a check to see that the protons stopped in the chamber. In the second configuration the absorber was increased to a thickness sufficient to stop the most energetic protons. In each configuration runs were taken with both empty and filled target cells. The results from the two configurations were combined in the analysis to yield complete coverage of the photon energy range between 180 and 320 MeV.

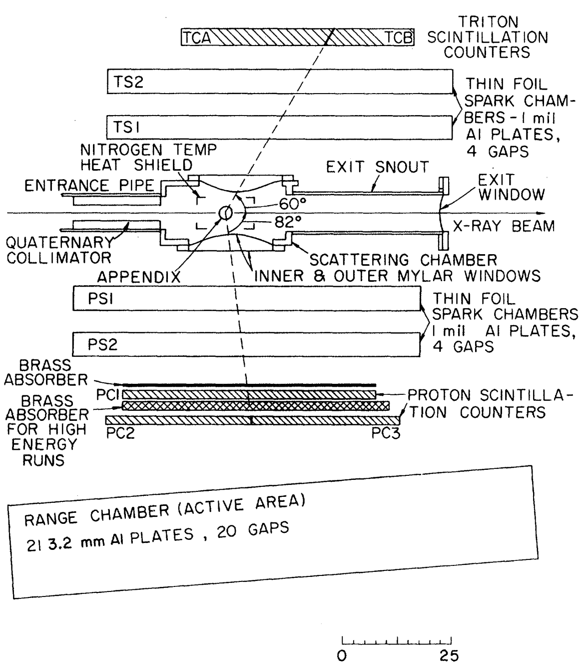

FIG. 1. Experimental arrangement.

DATA REDUCTION

Approximately 27 000 frames were recorded in the course of the experimental runs. These frames were scanned for the characteristic "signature" of a $^4\mathrm{He}(\gamma, p)t$ event. The scanners searched for two prong tracks in which the particle entering the protns detection appratus stopped in the thick-plate spark chamber. Frames which fit this description were also checked to see if the tracks were coplanar with each other and the

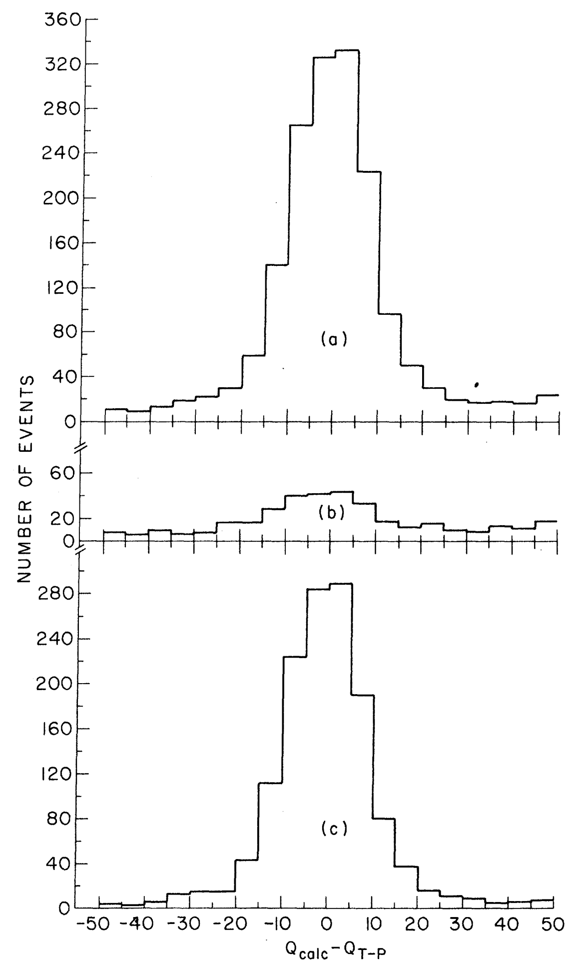

FIG. 2. Deviation of the experimentally determined Q's of the reaction from their known values. Q_{calc} is the reaction Q calculated from the energy and angle of the proton and the angle of the triton. Q_{T-P} is the known value of Q for $^4\mathrm{He}(\gamma, p)t$ (19.8 MeV). Distribution (a) is for all events, (b) is for events which were more than 1.75° out of coplanarity, and (c) is for events which were coplanar within 1.75°.

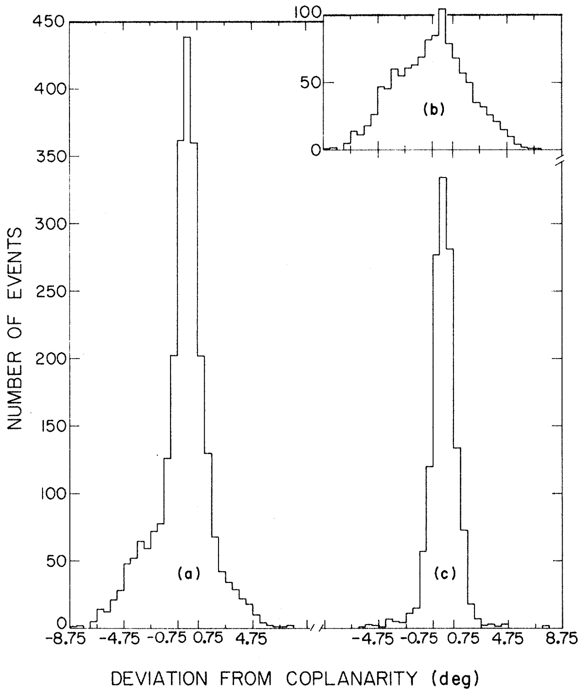

FIG. 3. Observed deviation from coplanarity of the recorded events. Distributions (a) is for all events. Distribution (b) is for events whose calculated Q differed from the expected Q for ^{4}He(γ, p)^{3}H by more than 15 MeV. Distribution (c) is for events whose Q was within 15 MeV of the expected Q.

beam line. This test was facilitated by the mirror view of the chambers, which placed the virtual camera position on the beam line slightly below beam height. In this view, coplanar tracks appeared as almost a single straight line. Using a template, the scanners selected those frames in which the mirror view of the triton chamber track was colinear with proton thin-foil chamber track within ±4.0°. The scan produced 2513 frames deemed worthy of measurement.

The frames selected by the scan were measured on a Hydel film measuring machine, and the tracks were reconstructed in space by a computer program. The angles of the particles were determined from their tracks in the thin-foil chambers, and the range of the proton was calculated from its trajectory and stopping point in the thick-plate chamber. A range-energy table contained in the program calculated the energy of the proton from its range.

The measured energy and angle of the proton and the angle of the triton were sufficient for a one constraint fit to the two body kinematics. In order to check the consistency of the measurement, they were used to determine a Q value for the reaction. The difference between the measured Q value and the known Q (19.8 MeV) is shown in Fig. 2. It represents a measure of the uncertainty in the energy involved in the reaction and is approximately the uncertainty in the photon energy.

Those events whose Q deviated less than 15 MeV from the Q for a ^{4}He(γ,p)t event were accepted. Those events which met this criterion were additionally required to be coplanar within ±1.75°. Figure 3 shows the deviation from coplanarity of the measured events. The assymmetry of the distribution in Fig. 3 was caused by the fact that the virtual camera position was slightly below the beam line.

The events with satisfactory Q and coplanarity were further checked to see if the origin of the event, as indicated by the point of closest approach of the triton and proton trajectories, lay within the target cell area. Less than 1% of the events were eliminated by this criterion and they were considered spurious. Calculations based on a Gaussian form for the distributions in Figs. 2(a) and 3(c) indicated that the 15-MeV Q deviation cutoff removed 7% of the good events, while the ±1.75° coplanarity requirement removed an additional 2%. Corrections were made for these losses.

Pictures taken during runs in which the target was evacuated were processed in the same way as the pictures taken during the data runs. The empty target runs taken in the first absorber con-

TABLE I. Differential cross sections in the center-of-mass system for ^{4}He(γ,p)^{3}H in units of 10^{-32}cm^2/sr. The errors shown are based on counting statistics only.

Energy (MeV)	cos θ^* −0.4	−0.2	0.	0.2	0.4
190	16.1 ± 3.4	35.4 ± 5.1	45.7 ± 5.8	70.2 ± 7.2	75.6 ± 7.7
210	10.8 ± 3.0	21.9 ± 4.3	41.7 ± 6.0	62.0 ± 7.3	103.6 ± 9.5
230	10.5 ± 3.2	12.6 ± 3.5	18.6 ± 4.3	31.8 ± 5.6	52.4 ± 7.3
250	6.5 ± 2.6	6.6 ± 2.7	7.8 ± 2.9	26.0 ± 5.4	61.4 ± 8.4
270	3.6 ± 2.1	4.1 ± 2.1	13.5 ± 3.9	10.2 ± 3.2	47.2 ± 7.7
290	4.6 ± 2.7	6.8 ± 2.6	5.9 ± 2.1	4.7 ± 1.7	20.0 ± 3.5
310	1.3 ± 0.9	6.3 ± 2.2	4.8 ± 2.0	3.3 ± 1.6	13.5 ± 3.4

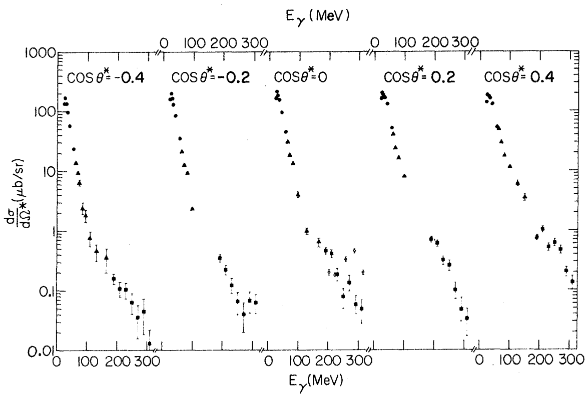

FIG. 4. Experimental differential cross sections. The closed circles are data of Gorbunov, closed triangles are from Stenberg, closed squares are from this experiment, and open diamonds are from Picozza *et al.* The cross sections and angles are in the c.m. system.

figuration produced 128 frames, of which only one passed all criteria as a valid ${}^4\mathrm{He}(\gamma,p)t$ event. In an equivalent run with a full target one expected 100 good events. The empty target runs in the second absorber configuration produced 185 pictures and none passed all the criteria. Because the background was small compared with the other corrections, no background substraction was made.

The 997 events selected as ${}^4\mathrm{He}(\gamma,p)t$ events were binned according to photon energy and c.m. proton angles and the cross sections were obtained. The largest correction to the cross sections was for the loss of protons via inelastic nuclear interactions in the absorbing material. The fraction of protons lost was calculated from the tables of Measday and Richard-Serre.[6] This loss ranged from 13% of the protons in the bin at $\cos\theta^* = -0.4$ and $E_\gamma = 190$ MeV to 32% in the bin at $\cos\theta^* = 0.4$ and $E_\gamma = 310$ MeV. Corrections were also made for the overlap in coverage of the runs made with the two absorber configurations. Since the observed efficiency of the spark chambers and scintillation counters was better than 99%, no correction was applied for detector efficiency. The resulting calculated cross sections are listed in Table I.

Figure 4 shows the variation of the cross section with energy at five angles. The general trend at all angles appears to be an exponential decline of the cross section with increasing photon energy. We see no evidence of an enhancement in the neighborhood of the first pion-nucleon resonance, such as that reported by Picozza *et al.*[5] Since Picozza *et al.* measured only at 90°, no comparison can be made with our results at the other angles.

A least-squares fit to the data with the expression

$$\frac{d\sigma}{d\Omega^*} = A\sin^2\theta^*(1+\beta\cos\theta^* + \gamma\cos^2\theta^*), \qquad (1)$$

where θ^* is the proton emission angle in the c.m. system, was performed at each photon energy. The best fit values for the parameters are given in Table II. While this form is the same as that for the first three terms of the electric multipole expansion, one cannot expect a three-term expansion to be valid in this energy region, and interpretation of these parameters as representing the values of the coefficients of the expansion is probably unwarranted. It was used in order to facilitate comparison with the results of other experiments in which this form was also used to represent the angular distribution. The calculated angular distributions and experimental points for the various photon energies are shown in Fig. 5.

The angular distributions observed in this experiment display the same general features as those observed at lower energies by Gorbunov[3] and Stenberg.[4] There is a forward peaking of the differential cross section and this forward peaking increases with increasing photon energy. The angular distributions for energies above 250 MeV seem to show evidence of a more complicated structure. In particular the points at $\cos^{-1}(0.2)$ are depressed relative to the 90° points.

TABLE II. Total cross section, χ^2, and parameters calculated for fits to the angular distribution $d\sigma/d\Omega^* = A\sin^2\theta^*[1+\beta\cos\theta^*+\gamma\cos^2\theta^*]$. The errors are calculated from the statistical errors of the experimental data.

Energy (MeV)	A (cm²/sr)	β	γ	χ^2	Calculated total cross section (μb)
190	$(5.0\pm0.9)\times10^{-31}$	1.8 ± 0.45	0.8 ± 1.9	1.28	4.8 ± 1.7
210	$(4.0\pm0.9)\times10^{-31}$	3.1 ± 0.9	3.7 ± 2.7	1.67	5.9 ± 1.9
230	$(1.9\pm0.6)\times10^{-31}$	3.0 ± 1.2	5.6 ± 4.0	0.378	3.4 ± 1.2
250	$(1.0\pm0.4)\times10^{-31}$	6.7 ± 3.1	16.3 ± 9.0	3.87	3.6 ± 1.1
270	$(7.8\pm4.3)\times10^{-32}$	4.7 ± 3.1	10.0 ± 10.0	12.94	1.9 ± 1.1
290	$(4.0\pm2.8)\times10^{-32}$	2.7 ± 2.3	12.0 ± 13.0	9.52	1.1 ± 0.7
310	$(4.1\pm3.7)\times10^{-32}$	2.1 ± 1.9	2.0 ± 12.0	8.75	0.5 ± 0.8

INTERPRETATION

Although there have been a number of calculations of the cross section for energies below 100 MeV [1] these are not valid at energies as high as those involved in this experiment. A calculation by Dzhibuti and Tagviashvili[7] was successful in reproducing some features of the cross section up to an energy of 150 MeV. These authors considered ^{4}He as a two-body system consisting of a proton moving in the field of a triton. Gaussian wave functions were used and cross sections were calculated without expanding the electromagnetic field into multipoles. Didelez *et al.*[2] made specific calculations for their energy using Gaussian and Irving wave functions.

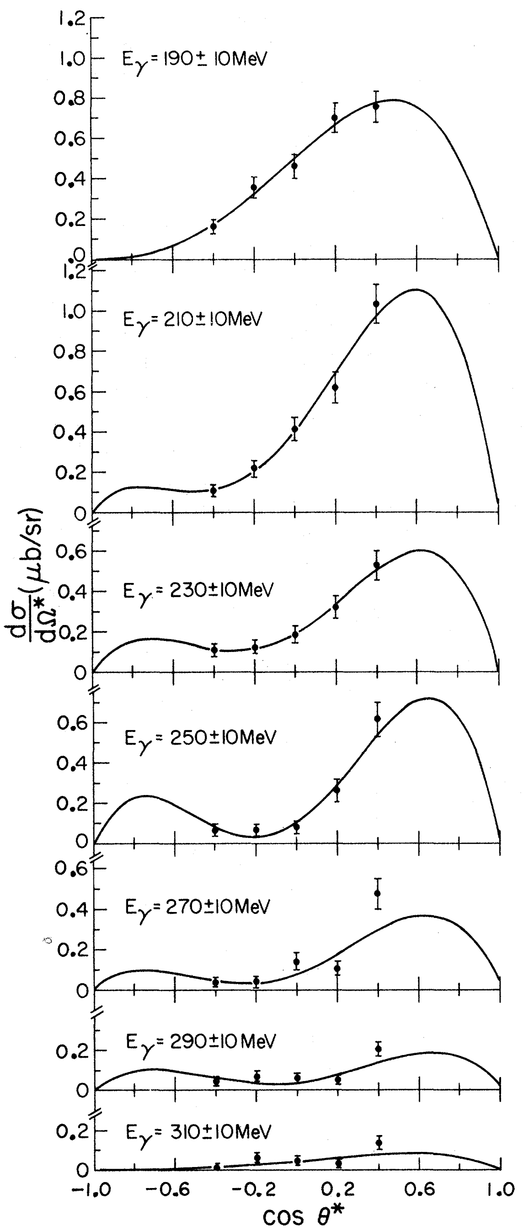

FIG. 5. Experimental differential cross sections and fitted angular distributions for various energies. The curves are least-squares fits of $d\sigma/d\Omega^* = A\sin^2\theta^*[1+\beta\cos\theta^*+\gamma\cos^2\theta^*]$ to the data. The cross sections and angles are in the c.m. system.

At high energies it is known that this particular two-body reaction, ^{4}He$(\gamma,p)t$, represents a very small fraction of the events initiated by a high-energy photon. The total cross section for the reaction at 300 MeV is only about 1 μb as compared to cross sections of 200 μb for pion production from each nucleon. The cross section is also very small compared to the total cross section for the ejection of protons by the quasideuteron effect.[8]

In a qualitative way the ejection of a proton from ^{4}He without breaking up the remaining triton can be imagined as requiring two conditions. First, the internal momentum components of the

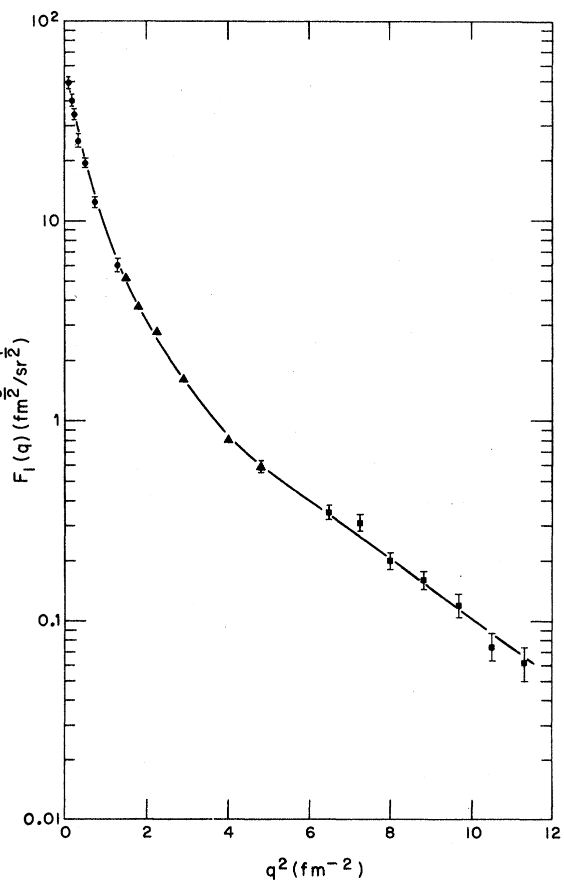

FIG. 6. Values of $F_1(q^2)$ calculated from the experimantal cross sections. The line is a smooth curve drawn through the points.

^{4}He nucleus must permit a proton to leave in one direction and the center of mass of the remaining three mucleons in the opposite direction while conserving energy and momentum as the photon is absorbed. Second, the momentum configuration of the three nucleons in their own rest frame must approximate that of a triton sufficiently for a real triton to appear in the final state.

In what follows we attempt to isolate a function of the momentum of the nucleons in the nucleus which gives the dominant dependence of the cross section on the energy. Since it has not been possible to find wave functions of helium which adequately represent the momentum distributions involved in the reaction at high energies, we will avoid the explicit use of wave functions except for the calculations of the less critical parts of the reaction. Instead we will utilize the 90° experimental cross section points to determine the function of momentum. In turn, we will use this empirically determined function to compute the value of the cross section at angles other than 90°. We will use a formula for the cross section based on the following assumptions.

We assume that the ^{4}He and ^{3}H wave functions are spatially symmetric S states, composed of nucleons with zero orbital angular momentum with respect to the center of mass of the nuclei, and that the motion of the outgoing proton and triton can be represented by plane waves. We include both electric and magnetic interactions in our calculations. In the electric interaction, we assume that the nuclear current is just the convection current due to the motion of the nucleons. The magnetic interaction is assumed to be that associated with the free magnetic moments of the individual nucleons. We neglect final state interactions. Under these conditions, the resulting formula for the cross section in the center of momentum system is[9]

$$\frac{d\sigma}{d\Omega^*}=\frac{3}{(8\pi)^2}\alpha\lambda_C\frac{k_p{}^3}{k_\gamma}\left\{\sin^2\theta^*[F_1(q_1)-\tfrac{1}{3}F_2(\vec{q}_2,\vec{k}_\gamma)]^2+\frac{\mu_p{}^2k_\gamma{}^2}{2k_p{}^2}[F_1(q_1)-F_2(\vec{q}_2,\vec{k}_\gamma)]^2\right\}. \tag{2}$$

The quantity α is the fine structure constant, λ_C is the Compton wavelength of the proton, μ_p is the magnetic moment of the proton, $\hbar k_p$ is the c.m. momentum of the proton, $\hbar k_\gamma$ is the c.m. momentum of the photon, and θ is the proton emission angle in the c.m. system. The functions F_1 and F_2 are defined as

$$F_1(q)=\int d^3y_1d^3y_2d^3y_3\exp(-i\vec{q}\cdot\vec{y}_1)U_4(\vec{y}_1,\vec{y}_2,\vec{y}_3)U_3^*(\vec{y}_2,\vec{y}_3) \tag{3}$$

and

$$F_2(q,k_\gamma)=\int d^3y_1d^3y_2d^3y_3\exp(-i\vec{q}\cdot\vec{y}_1)\exp(\tfrac{1}{3}i\,2\vec{k}_y\cdot\vec{y}_2)U_4(\vec{y}_1,\vec{y}_2,\vec{y}_3)U_3^*(\vec{y}_2,\vec{y}_3); \tag{4}$$

while their arguments, q_1 and q_2, in Eq. (2) are

$$\vec{q}_1=\vec{k}_p-\tfrac{3}{4}\vec{k}_\gamma,$$
$$\vec{q}_2=\vec{k}_p+\tfrac{1}{4}\vec{k}_\gamma.$$

U_3 is the spatial part of the ^{3}H wave function, and U_4 is the spatial part of the ^{4}He wave function. The coordinates $\vec{y}_1$, $\vec{y}_2$, and $\vec{y}_3$ are internal coordinates of the ^{4}He nucleus defined in terms of the coordinates of the individual nucleons as

$$\vec{y}_1=\vec{x}_1-\tfrac{1}{3}(\vec{x}_2+\vec{x}_3+\vec{x}_4),$$
$$\vec{y}_2=\vec{x}_2-\tfrac{1}{2}(\vec{x}_3+\vec{x}_4),$$
$$\vec{y}_3=\vec{x}_3-\vec{x}_4.$$

The cross section in Eq. (2) is determined by the two functions F_1 and F_2. $F_1(q)$ is the probability amplitude for finding a proton with momentum $\hbar\vec{q}$ in the ^{4}He nucleus weighted by the overlap between the ^{4}He and ^{3}H wave functions. F_2 is a similar function representing the amplitude associated with the recoiling three-body system. The first term in Eq. 2, involving $\sin^2\theta^*$, comes from the electric interaction. The other term comes from the magnetic interaction. The quantity $\hbar\vec{q}_1$ is the momentum of the proton relative to the c.m. of the ^{4}He nucleus before the interaction with the photon. The quantity $\hbar\vec{q}_2$ is the momentum of the center of mass of the three nucleon system relative to the c.m. of the ^{4}He nucleus before it interacts with the photon.

The calculation of F_1 and F_2 requires specification of both the ^{4}He and ^{3}H wave functions. However, if we calculate only the angular distribution rather than the magnitude of the cross section, we can proceed with considerably less information. Our aim is to find an approximate relationship between F_1 and F_2. In particular, we would like to be able to write $F_2(\vec{q}, \vec{k}_\gamma) = F_1(q) f(k_\gamma)$.

In order to obtain this approximate relationship between F_1 and F_2, we rewrite Eq. (4) in a form involving the form factor $f(\vec{y}_1, \vec{k}_\gamma)$ for the transition from the initial three nucleon configuration in the ^{4}He nucleus to the final-state triton, where

$$f(\vec{y}_1, \vec{k}_\gamma) = \frac{\int U_4(\vec{y}_1, \vec{y}_2, \vec{y}_3) U_3^*(\vec{y}_2, \vec{y}_3) \exp(\tfrac{1}{3} i 2\vec{k}_\gamma \cdot \vec{y}_2) d^3y_2 d^3y_3}{\int U_4(\vec{y}_1, \vec{y}_2, \vec{y}_3) U_3^*(\vec{y}_2, \vec{y}_3) d^3y_2 d^3y_3} \tag{5}$$

is normalized to unity at $k_\gamma = 0$. Now Eq. (4) becomes

$$F_2(\vec{q}, \vec{k}_\gamma) = \int e^{-i\vec{q}\cdot\vec{y}_1} U_4(\vec{y}_1, \vec{y}_2, \vec{y}_3) U_3^*(\vec{y}_2, \vec{y}_3) f(\vec{y}_1, \vec{k}_\gamma) d^3y_1 d^3y_2 d^3y_3 . \tag{6}$$

The dependence of f on $\vec{y}_1$ arises from the correlation between the initial three-nucleon configuration and the position of the other nucleon. If it were not for its $\vec{y}_1$ dependence, the transition form factor f could be removed from the integral for F_2, and F_2 would be the desired product.

We can see from Eq. (5) that only the initial states which have a substantial overlap with the final triton wave function will contribute significantly to F_2. This means that the initial three-nucleon configuration must be somewhat similar to a triton. Furthermore, the momentum transfer involved is not very large, since k_γ^2 is less than 2.6 fm^{-2} even at 310 MeV. At these low values of momentum transfer, the ^{3}H form factor is essentially determined by the rms radius.

As an approximation, we will replace $f(\vec{y}_1, \vec{k}_\gamma)$ in Eq. (6) by its average defined as

$$\bar{f}(k_\gamma^2) = \int U_4^* f(\vec{y}_1, \vec{k}_\gamma) U_4 d^3y_1 d^3y_2 d^3y_3 .$$

Values of $\bar{f}(k_\gamma^2)$ are calculated from Eq. (5) using ^{4}He and ^{3}H wave functions which agree with measured form factors at low momentum transfer.

For calculational convenience, we have used Gaussian wave functions adjusted to fit the matter form factors for ^{4}He and ^{3}H in the computation of $\bar{f}$. In this case, we have

$$\bar{f}(k_\gamma^2) = e^{-0.362 k_\gamma^2} , \tag{7}$$

where k_γ is in inverse fermis. We can then write Eq. (6) as

$$F_2(\vec{q}, \vec{k}_\gamma) = e^{-0.362 k_\gamma^2} F_1(q) . \tag{8}$$

Substituting Eq. (8) in Eq. (2) we have a formula involving F_1 only,

$$\frac{d\sigma}{d\Omega^*} = \frac{3\alpha\lambda_C}{(8\pi)^2} \frac{k_p^3}{k_\gamma} \left\{ \sin^2(\theta^*)[F_1(q_1) - F_1(q_2)\tfrac{1}{3} e^{-0.362 k_\gamma^2}]^2 + \frac{\mu_p^2}{2} \frac{k_\gamma^2}{k_p^2} [F_1(q_1) - F_1(q_2) e^{-0.362 k_\gamma^2}]^2 \right\} . \tag{9}$$

Although we now have a single function F_1, it appears in the equation with two different arguments, q_1 and q_2. If we can find a condition such that $q_1 = q_2$ it will be possible to determine F_1 from experimental cross sections. Noting that

$$q_1^2 = k_p^2 - \tfrac{3}{2} k_p k_\gamma \cos\theta^* + \tfrac{9}{16} k_\gamma^2$$

and

$$q_2^2 = k_p^2 + \tfrac{1}{2} k_p k_\gamma \cos\theta^* + \tfrac{1}{16} k_\gamma^2 ,$$

we see that the condition for q_1 to be equal to q_2 is that

$$\cos\theta^* = k_\gamma / (4 k_p) .$$

At this angle, which we call θ', we have

$$\frac{d\sigma}{d\Omega}(\theta') = \frac{3\alpha\lambda_C}{(8\pi)^2} \frac{k_p^3}{k_\gamma} F_1^2(q(\theta')) \left\{ \sin^2(\theta')[1 - \tfrac{1}{3} e^{-0.362 k_\gamma^2}]^2 + \frac{\mu_p^2}{2} \frac{k_\gamma^2}{k_p^2} [1 - e^{-0.362 k_\gamma^2}]^2 \right\} . \tag{10}$$

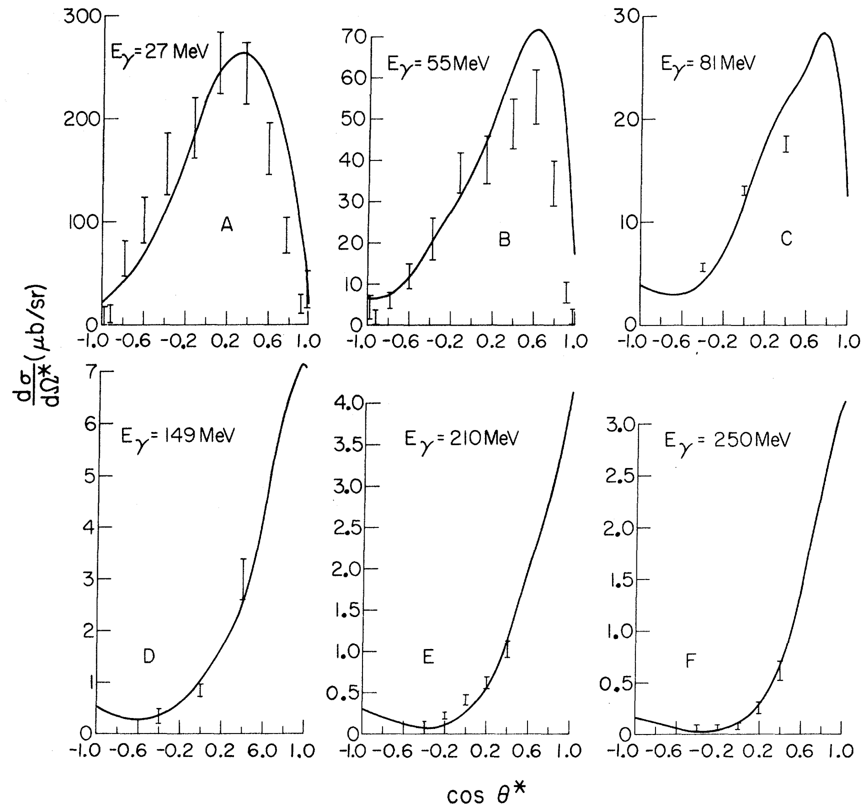

FIG. 7. Angular distributions calculated from $F_1(q^2)$. The points in (a) and (b) are from the data of Gorbunov, (c) and (d) are from Stenberg, and (e) and (f) are from this experiment.

The angle θ' varies between $\cos^{-1}(0.05)$ and $\cos^{-1}(0.1)$ for photon energies between 25 and 300 MeV.

The function $F_1(q)$ can now be determined using the experimental values of the cross section at the angle θ' for each energy. Although experimental measurements were not available at these exact angles, extensive measurements are available close to 90°. Reliable extrapolations from the data near 90° to the angles θ' were made using the parametrization indicated in Eq. (1). The values of the function $F_1(q)$ obtained from this procedure are shown in Fig. 6. This function is then used to calculate the cross section at other angles by means of Eq. (9).

The results of this calculation for six photon energies are given in Fig. 7 along with experimental measurements at those energies. The agreement with the experimental points appears to be reasonably good. The increasing forward peaking of the cross section with energy is well reproduced, although this peaking seems exaggerated at all energies. Clearly, comparison with the as yet unmeasured high energy cross sections near 0 and 180° would provide a more severe test of the usefulness of this type of calculation.

SUMMARY AND CONCLUDING REMARKS

The cross sections measured in this experiment show a basic continuity with the results at lower energies. There is the same exponential decline of the cross section with energy and a continuation of the forward peaking of the proton angular distribution. We have been able to produce a satisfactory fit to our angular distributions with a semiempirical function of the internal momenta of the ^{4}He nucleus. Our results do not show the pronounced rise in the 90° cross section reported in Ref. 3. Further measurements including some near 0 and 180° will be particularly valuable in deciding on the validity of the model and on the relative importance of the magnetic and charge contributions.

Note added: A preliminary report on measurements with protons up to 450 MeV at 60 and 90° indicate cross sections which decrease continuously but less rapidly with energy than our measurements.[10]

ACKNOWLEDGMENTS

The authors wish to thank Professor Albert Wattenberg for the use of a number of spark chambers, Dr. John Staples and Don Vermillion for the engineering and operation of the betatron, and Scott Wetenkamp, Parviz Moarefi, Bijan Parhami, and David Fancher for assistance in the construction of apparatus and collection of the data. One of us (S.E.K) wishes to thank Dr. Donald Lehmann of the National Bureau of Standards and Dr. Ben Gibson of Los Alamos Scientific Laboratory for helpful discussions on some aspects of the calculations. The interest and advice of Professor R. L. Schult and Professor D. G. Ravenhall regarding the interpretation of the experiment are especially appreciated.

---

*Supported in part by the National Science Foundation.
†Present address: Lawrence Livermore Laboratory, Livermore, California 94550.

[1]W. E. Meyerhof and S. Fiarman, Photodisintegration of Helium 4. This is a review which will appear in the Proceedings of the Asilomar International Conference on Photonuclear Reactions and Applications, held 26 March 1973. See also S. Fiarman and W. E. Meyerhof, Nucl. Phys. (to be published).

[2]J. P. Didelez, H. Langevin-Joliot, N. Bijedic, and Z. Maric, Nuovo Cimento **67A**, 388 (1970).

[3]A. N. Gorbunov, Phys. Lett. **27B**, 436 (1968).

[4]C. G. Stenberg, Ph.D. thesis, University of Illinois, 1968 (unpublished).

[5]P. Picozza, C. Schaerf, R. Scrimaglio, G. Goggi, A. Piazzoli, and D. Scanniechio, Nucl. Phys. **A157**, 190 (1970).

[6]D. F. Measday and C. Richard-Serre, Nucl. Instrum. Methods **76**, 45 (1969).

[7]R. I. Dzhibuti and A. V. Tagviashvili, Zh. Eksp. Teor. Fiz. **39**, 1756 (1960) [transl.: Sov. Phys.–JETP **12**, 1225 (1961)].

[8]M. Q. Barton and J. H. Smith, Phys. Rev. **110**, 1143 (1958).

[9]S. E. Kiergan, Technical Report No. 192, Physics Research Laboratory, University of Illinois, 1972 (unpublished), Appendix.

[10]Claude Schuhl, Saclay, France, private communication.